Non-Gaussian effects in $1/f$ noise in small silicon-on-sapphire resistors

P. J. Restle, R. J. Hamilton, M. B. Weissman, and M. S. Love
Department of Physics, University of Illinois at Urbana-Champaign, 1110 West Green Street, Urbana, Illinois 61801
(Received 27 July 1984)

Several models for $1/f$ noise in silicon which give identical predictions for noise spectra were found to give distinct predictions for non-Gaussian effects as shown by Monte Carlo simulations. Measurements on silicon-on-sapphire resistors ranging in area to less than 1 $(\mu m)^2$ revealed both non-Gaussian effects and sample-to-sample spectral variations. The results were qualitatively similar to those expected for a simple superposition of two-level trapping systems and dissimilar to those for a random walk in a random potential. However, some random modulation of some of the two-level systems was found.

INTRODUCTION

Recently, substantial progress has been made toward understanding $1/f$ noise in semiconductors, particularly silicon. As we shall discuss, the evidence now points strongly toward fluctuating occupancy of traps as the principle noise mechanism, with the $1/f$ kinetics arising from a spread of activation energies of some not yet characterized processes.[1,2] The activation could conceivably involve intermediate electronic states in the trapping process, a tight coupling of the trapping to some atomic motion, or a weak coupling of trap depths to some activated atomic motions. A somewhat more interesting, if vague, possibility is that a perpetual wandering of the glassy surface oxide interface among a huge set of low-lying configurational states might give something like a "random walk in a random potential" (RWRP) which can give $1/f$-like noise for rather fundamental reasons.[3,4] In this paper we examine higher-order effects in the noise voltage, beyond the standard two-point correlations or spectra, in very small silicon-on-sapphire (SOS) resistors to attempt to resolve these questions.

Although there is now a plethora of work implicating trapping, particularly surface trapping, in semiconductor $1/f$ noise,[5] we shall briefly review some of the more convincing recent pieces of evidence. In metal-oxide-semiconductor (MOS) transistors the surface trapping state density may be varied over a wide range, and the noise magnitude varies with it.[6] In silicon wafers (Ref. 7) and SOS (Ref. 1) the resistivity fluctuations are approximately scalar, as expected for trapping. The magnitude of the Hall coefficient noise in SOS fits a trapping model and, as would be expected, these fluctuations are almost completely correlated with the resistivity fluctuations.[1] In HgCdTe, surface cleaning under vacuum removes low-frequency noise preferentially,[8] until the surface oxide regrows, as expected for tunneling trapping kinetics or perhaps for glassy rearrangement kinetics if the characteristic times are size dependent. Most relevant to this work, in submicron silicon metal-oxide-semiconductor field-effect transistors individual two-level systems, apparently single traps, with a range of characteristic times which might lead to $1/f$ noise, have been found.[2]

EXPERIMENTAL IMPLICATIONS OF MODELS

There are several frameworks for models of $1/f$ noise with activated kinetics. The simplest is that of Dutta and Horn,[9] in which the noise arises from many independent two-state systems, with level spacings not much bigger than kT and with activation energies many times kT having enough spread to give nearly $1/f$ noise. Such a model makes no detailed predictions about the spectral shape, but does predict a relation between the spectral shape and the temperature dependence of the noise magnitude which has been qualitatively confirmed in many systems. At an opposite limit, Marinari *et al.*[4] have proposed a model in which the thermally activated transitions are not independent but rather linked into a random topography in some low-dimensional configuration space, giving a random potential. To the extent that this theory is taken literally in its original scale-similar form, it predicts simpler spectral shapes than are actually found. If the Fourier spectrum of the random potential is made somewhat adjustable, realistic spectra may be obtained. However, the theory relating the spectral shape to the temperature dependence seems to be formally identical to that for a Dutta-Horn model, so that the relation between these quantities cannot be used to discriminate between the two models.[10]

One may easily see that various non-Gaussian properties (i.e., statistical properties involving higher-order than second correlation functions)[9,11] are quite different between the Dutta-Horn model and an RWRP model. For samples so small that only a small number of two-state systems would be found with characteristic frequencies in any octave, the Dutta-Horn model clearly would predict sample-to-sample variation in the frequency spectrum, due to random fluctuations in sampling from the net distribution of activation energies. In addition there are more subtle non-Gaussian effects which we have studied by Monte Carlo simulations, as discussed below. In contrast, in an RWRP model the noise in some octave is determined not by the initial draw of two-state systems but rather by the detailed shape of a particular potential valley (of the appropriate scale) in which the configuration happens to be found. It is inherent in the RWRP description that the noise in lower octaves comes from the

slower wandering between different valleys of this scale. Thus the sort of variations in spectral density which appear between members of an ensemble in the Dutta-Horn model appear in a single sample as a function of time in an RWRP model. By looking at samples small enough so that sample-to-sample variations and/or single-sample non-Gaussian effects are apparent, one should be able to distinguish between the two types of models.

In fact, as we shall see in the data, the Dutta-Horn relation between the spectral shape and the temperature dependence is not expected to directly apply to trapping noise in semiconductors. Since the Fermi level is temperature dependent and since most of the fluctuations come from traps near the Fermi level, at different temperatures one sees different collections of traps. (This complication arises because there is a large entropy difference between the trapped and untrapped states, unlike ordinary glassy two-state systems.) Nevertheless, not only the overall noise magnitude but also the magnitude of features is roughly independent of temperature.[1] The obvious interpretation is that the kinetic parameters are not strongly correlated with trap depth,[1] and that the density of states of the traps is not strongly peaked. However, in samples so small as to show random sample-to-sample spectral shape variations, one would expect that random correlations might appear between kinetic parameters and trap depths. In other words, if the noise in some octave came from a small number of traps they would not ordinarily by chance have depths evenly distributed about the Fermi level, so that bumps in the spectrum would show anomalous temperature dependences of their sizes.

All of the non-Gaussian effects, sample-to-sample variations, and anomalous temperature dependences of features predicted for two-state system models would be expected for samples in the size range of our samples only if one two-state transition either directly corresponds to a trapping event or to a significant change in the trapping probability of a fast trap. For transitions weakly coupled to trap depths (a model some of us at one point suggested[1]) these effects would be much smaller and, for the anomalous temperature dependences, qualitatively different. If each of a small number of traps gave noise reflecting the kinetics of several two-state systems, the anomalous temperature dependence would be found for each feature from those systems rather than for single features.

STATISTICAL TESTS

In principle one can find an infinite number of multipoint correlation functions which contain information not found in the spectrum or two-point correlation. Our choice of functions to examine was guided partly by intuition as to what functions would be sensitive to finite numbers of two-level systems, partly by limitations of an early version of the data-gathering setup, in which the computer had access only to power spectra and not the original voltages,[11] and partly by effects observed during the experiments. Several of our statistical parameters have been described in detail elsewhere.[12]

Ordinary 512-point fast-Fourier-transform (FFT) power spectra from 1024 voltage points were taken and summed by octave. Each octave contained between 1 and 128 discrete Fourier bands. An additional half-octave containing bands 257—362 was also used. Bands 363—512 were not used because of effects of the antialias filters. The variances and covariances of these noise powers per octave were taken.[12] For Gaussian noise there are simple predictions for the variances and even simpler (zero) predictions for the covariances, with predictable standard deviations of the values after finite sampling.[12] The on-diagonal elements (variances) of the covariance matrices shown below are normalized so that Gaussian noise would give 1.0, independent of spectral shape—a slightly different normalization than used previously.[12] The off-diagonal elements are simply correlation coefficients. Histograms of the noise power in each octave were also taken—these served primarily to allow for detection of occasional artifacts.[12]

Finally, a time series of power per octave values were taken, then Fourier transformed to give a type of four-point spectrum. These spectra served to characterize the time course of the power variations and turned out to be useful in distinguishing different types of non-Gaussianity. Since a single input point to this "second spectrum" requires taking an entire ordinary spectrum (from 1024 voltage points) accumulation of reasonably good statistics requires about 10^3 times longer for the second spectrum than for the ordinary one.

MONTE CARLO SIMULATIONS

A variety of increasingly complex simulations of the behavior of superposed two-state systems were made. In each case each system was assigned a characteristic relaxation time, amplitude, and duty cycle (fraction of time in, for example, the "up" state) and these quantities remained fixed for the duration of the simulation. Random number generators of the computers (an LSI/model no. 11/23 equipped with a SKY array processor or, in most cases, a VAX 750) were used to determine flipping times independently for each system.

The simplest simulations were of single two-state systems. Results of a positive contribution to the diagonal terms of frequencies above the characteristic frequency of the two-state system and a slight negative contribution at frequencies near to the characteristic frequency were found consistently. For systems with duty cycles far from 0.5, the positive non-Gaussian contributions extended to frequencies close to the characteristic frequency. When single large systems were superimposed on a background (nearly Gaussian) of small systems, similar patterns appeared except, of course, that all the non-Gaussian effects due to the single system were diluted out by the background at frequencies far from the characteristic frequency.

In general those quantities (such as the diagonal elements of our covariance matrix) which can be represented as the expectation of some four-point product divided by the products of the expectations of some two-point products approach the Gaussian limit in a simple way. The non-Gaussian contributions to the numerator from each

independent contributing system just add, as do each of the two-point products in the denominator. Thus if one adds N independent systems, the non-Gaussianity is reduced by a factor of N. If one introduces a non-Gaussian source with spectral power r times that of a Gaussian background, the source's non-Gaussianity must be divided by $(1+r)^2$ to obtain the net non-Gaussianity. Thus, although the noise contributed by a single two-state system becomes increasingly non-Gaussian at frequencies above its characteristic frequency, in practice for a superposition of many such systems the non-Gaussianity (i.e., extra variance in the spectral density) peaks at frequencies slightly higher than the characteristic frequencies of each two-state system.

A large series of simulations were run in which collections of systems with random duty cycles and random characteristic frequencies were set up. The random characteristic frequencies were, of course, restricted to be within a range (of ten octaves) similar to that covered in the analyzed spectrum.

The probability density for the log of the characteristic frequency was chosen to be uniform, which corresponds to a $1/f$ expected spectrum. The random duty cycles were picked from the set

$$\left\{ \frac{1}{2^n+1}, \frac{2^n}{2^n+1} \;\middle|\; n=0,1,\ldots,7 \right\}$$

which corresponds to a discretized, truncated version of a uniform distribution of logarithms of ratios of "on" to "off" times. This distribution is especially appropriate to trapping models in which there is a flat distribution of trap depths.

Figure 1 shows four spectra from the same simulation algorithm, with 30 random systems with different random system parameters. As is expected and is typical for such system densities, substantial sample-to-sample variation appears in the spectra, which nevertheless remains generally of a $1/f$ form. Table I shows the covariance matrix for one of the simulations. Extra variance in the spectral power shows up in those regions in which the spectrum mostly arises from a small number of systems with characteristic frequencies below that of the observed band. The average diagonal term was about 8% higher than for Gaussian noise and the average interoctave correlation coefficient was about 0.07, or about 0.11 for adjacent octaves.

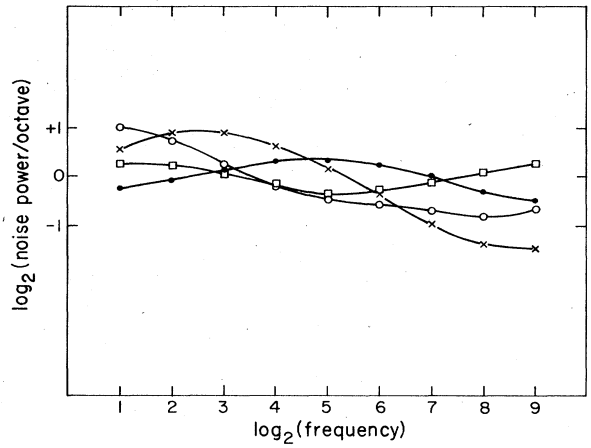

FIG. 1. Each octave spectrum shown was derived from the fluctuations of 30 two-state systems, with different randomly picked characteristic frequencies and duty cycles, as described in the text. Each spectrum has been normalized to the same net power so as to make the differences in spectral shape easier to judge.

Since, as we describe in the next section, some real samples showed more extra variance than was found in these simulations, we also tried simulations in which the sizes of the contributions from each system were also randomized, being picked from the set $\{1 \leq n \leq 5\}$ with probabilities $p(n) \propto e^{-n}$ to roughly simulate an exponential distribution. No qualitatively new features were found.

After one odd result appeared in the actual data—a dependence of the non-Gaussianity in a particular octave on the bandwidth (sampling rate) of the analyzer—we checked whether such an effect would appear in the simulations. A weak dependence of the diagonal variances on simulated sampling rates was found, but only in the lowest few octaves, with less than eight analysis bands per octave. Physically, this means that the frequency spectrum of the fluctuations in the noise power per octave was flat for frequencies below ~ 0.1 of the central frequency of the octave in the two-state simulations.

We also simulated the behavior of a one-dimensional RWRP. Higher dimensions were not used both for computational reasons and because there is some doubt as to whether they have any even theoretical relevance to $1/f$

TABLE I. Covariance matrix from the same simulation which appears as the dots in Fig. 1.

Octave	1	2	3	4	5	6	7	8	9
1	0.88								
2	0.04	1.07							
3	0.02	0.11	1.01						
4	0.04	0.06	0.05	0.99					
5	−0.01	0.00	−0.02	0.03	1.03				
6	−0.03	0.00	−0.01	0.04	0.06	1.12			
7	0.02	−0.02	0.03	−0.01	0.07	0.06	1.13		
8	−0.03	−0.01	−0.05	0.04	0.01	0.03	0.11	1.27	
9	0.04	−0.03	0.04	−0.02	0.04	0.01	0.09	0.11	1.36

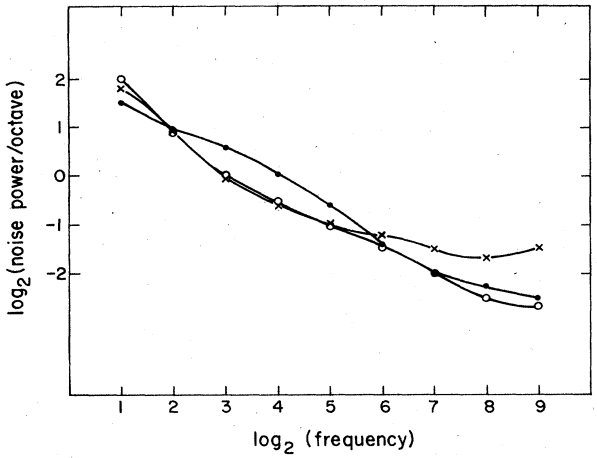

FIG. 2. Each of the three spectra shown is taken from a random walk in a different random potential. The sampling frequency is 0.01 of the maximum stepping frequency. Each spectrum is taken from the average square of 100 transforms of 1024 points. The apparent flattening at high frequencies is due to a form of aliasing.

noise.[13] The random potential was generated by randomly adding (usually) 0, 0.69, or -0.69 kT units for each step in position. To simplify computation, after 1000 steps the next zero crossing was identified with the first step, to give a periodic random potential. Scale similarity obviously holds only for diffusion distances less than this period. In practice, this restriction was not important. Starting positions of the random walker were picked randomly following a Boltzmann distribution. Each subsequent step also had Boltzmann-weighted probabilities. The random signal consisted then of the displacement of the random walker, taken directly, not modulo the periodicity.

At frequencies close to the single-step frequency, an RWRP does not show $1/f$ noise.[4] We found that the spectrum was reasonably close to $1/f$ (e.g., $f^{-1.5}$) at about $\frac{1}{100}$ of that frequency. Thus the position of the random walker was recorded after each 100 random moves. These simulations used an inordinate amount of computer time and therefore were not repeated with as wide a range of parameters as were used in the two-state-system simulations.

We did vary the size of the potential steps, using values of 0, 0.34, 0.69, 0.99, and 1.39. For large potential steps, the random walker was nearly always trapped, so that good statistics on its walk could not be obtained in a reasonable amount of computer time. For small step sizes, one has essentially free diffusion, with an f^{-2} spectrum, at frequencies above the inverse of the time required to diffuse far enough to see $\sim kT$ of structure in the potential. This frequency scales as the fourth power of the potential step size. Thus, making the step size much less than kT required allowing the random walker to make huge numbers of steps to approach the $1/f$ regime, which was also impractical.

The Monte Carlo results for the RWRP were dramatically different from those for the two-state systems. Variations in spectral shape between different random potentials were somewhat smaller than those found for the simulations with several two-state systems per octave, as can be seen by comparing Figs. 1 and 2. However, the spectral variances of individual potentials were typically many times the Gaussian value, with large variations between different potentials. A comparison of this value for three potentials constructed by the same algorithm gave values of 3.2, 38.2, and 7.3. An example of the covariance matrix for this last sample is shown in Table II. The interoctave correlation coefficients were very large and showed little variation, averaging 0.58. The average for adjacent octaves was 0.68.

The values for non-Gaussian variances and covariances in the two-state systems simulations with comparable spectral variation were much more than an order of magnitude smaller than the RWRP values.

SAMPLE PREPARATION

Ten samples were made from 5.6-mm squares of SOS donated by Hewlett-Packard. The epitaxially grown silicon with [100] orientation was 670-nm thick and very lightly doped (p-type, approximately 10^{13} cm^{-3}). A range of processing parameters were used to obtain a

TABLE II. Covariance matrix taken from 100 transforms of an RWRP, with the potential giving the dotted spectrum of Fig. 2. Two other sets of transforms gave similar results. Other random potentials gave widely varying diagonal terms. The normalization of the diagonal terms in this matrix is different from that of the other data and simulations by about 9%, which is negligible compared with the variation between simulations.

Octave	1	2	3	4	5	6	7	8	9
1	7.72								
2	0.46	5.18							
3	0.54	0.46	4.63						
4	0.22	0.42	0.63	5.69					
5	0.24	0.40	0.64	0.82	9.30				
6	0.13	0.30	0.59	0.74	0.85	12.51			
7	0.23	0.35	0.63	0.71	0.79	0.90	10.67		
8	0.35	0.33	0.51	0.43	0.52	0.51	0.63	6.22	
9	0.37	0.32	0.15	−0.09	−0.05	−0.10	0.00	0.53	6.71

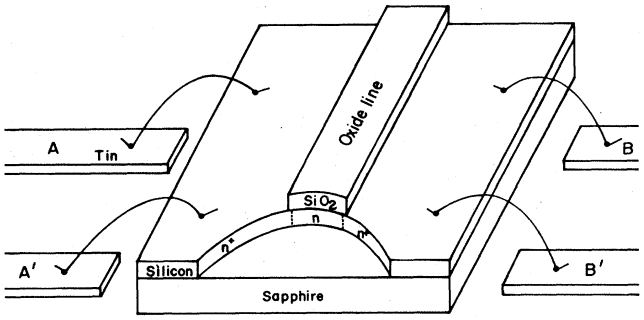

FIG. 3. Schematic diagram of the four probe samples is shown without the final passivating oxide layer. The silicon protected by the oxide line still has the original substate doping (p type $\sim 10^{13}$ cm^{-3}) except for the exposed edge surface which has been doped n type and has a surface area less than 1 μm^2 for most of the samples.

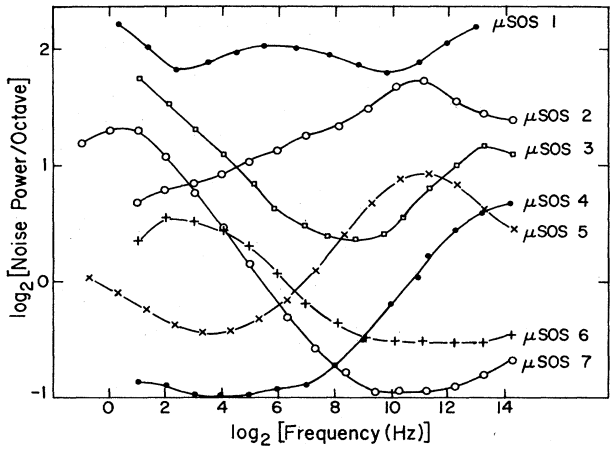

FIG. 4. Power spectra at room temperature for seven different samples having approximately the same size and geometry.

range of sample sizes, oxide thicknesses, and doping profiles. On a typical sample thermal oxidation was performed at 1100 °C for 10 to 168 min using wet oxidation, growing from 0.25 to 1.2 μm of oxide and leaving 0.56 to 0.15 μm of unoxidized silicon.

A photolithography mask having 5-μm lines of chrome was used with Shipley model no. AZ 1350T positive photoresist. To obtain thinner lines a double-exposure technique was sometimes used. The oxide was removed except for the line pattern. The unprotected regions were then doped with phosphorous at 1000 °C for 5 min, yielding $n > 10^{19}$ cm^{-3}. Several of the samples were then checked to make sure there was high resistance across the oxide lines.

Varying the processing parameters produced lines from 1 to 6 μm wide. Another mask was then used with photoresist and wet chemical etching to cut through the oxide line and the lightly doped silicon beneath it to expose an edge of the lightly doped silicon with a surface area of about 1 μm^2. The samples were again phosphorous—doped at around 670 °C for 5 min. Figure 3 shows a schematic diagram of the sample of this point in the processing. Then a final wet oxidation was performed at 920—1000 °C to grow a 0.1-μm passivating oxide. This process results in a central region doped with a profile[14]

$$n(x) \cong 10^{16} e^{-(x/0.04\,\mu\text{m})^2} - 10^{13}\ \text{cm}^{-3}$$

where x is the perpendicular distance from the oxide-silicon interface. The sample resistances were about 4 kΩ. Since the resistances before the final doping were greater than 10^6 Ω, the effects at the lightly doped p-type region are probably negligible. Separate current-carrying and voltage-sensing contacts were made with an ultrasonic aluminum lead bonder. The noise across each current and voltage pair of contacts was measured to ensure the contact noise was negligible.

METHODS

The current sources were standard batteries in series with wire-wound resistors having resistance greater than 20 times the sample resistance. Princeton Applied Research 113's were used for the differential amplification. Frequency Devices 7675 anti-alias filters and an ADAC model 1023AD analog-to-digital converter were used with a Digital Equipment Corp. LSI 11/23 computer to sample the noise voltage. A SKY array processor was used to perform the FFT's and other data manipulation. Some of the data were taken with an MMR Technologies nitrogen refrigerator with temperature range of 82 to 330 K.

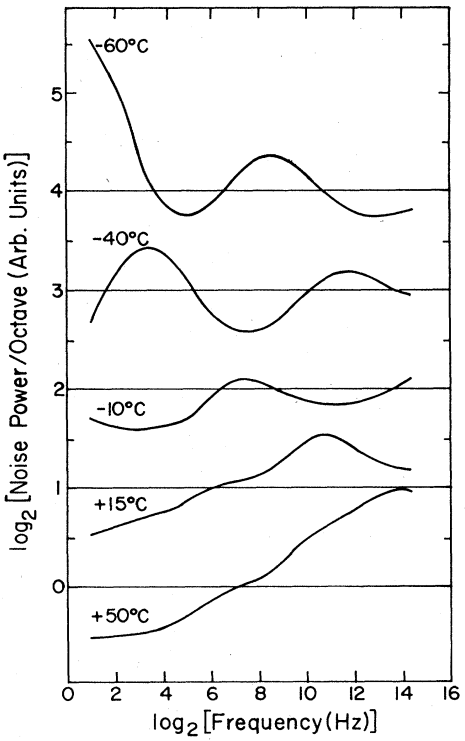

FIG. 5. Power spectra at five different temperatures for μSOS 4. The spectra were multiplied by 2 for every temperature step below 50 °C to prevent overlap on the figure.

TABLE III. Normalized covariance matrix for μSOS 7 measured from 1000 transforms. The frequency range covered is 53 Hz to 4.8 kHz.

Octave	4	5	6	7	8	9	10
4	1.14						
5	0.16	1.10					
6	0.09	0.10	1.14				
7	0.09	0.09	0.10	1.17			
8	0.00	0.07	−0.01	0.07	1.10		
9	0.10	0.05	−0.02	0.07	0.11	1.09	
10	−0.03	−0.07	−0.03	0.02	0.06	0.10	1.00

RESULTS

Power spectra were taken on all the samples at room temperature (Fig. 4). The spectra show greater deviations from the $1/f$ power law than larger samples,[1] and the spectral shapes show no correlation from sample to sample, even between samples that underwent identical processing on the same substrate.

Power spectra were taken at different temperatures for several samples. Figure 5 shows the data for one sample. The data clearly show thermally activated features, but unlike larger samples[1] the shape of the spectrum does not remain approximately constant. Figure 5 clearly shows a peak whose magnitude decreases with temperature, while other data show peaks that grow with temperature.

Data for the covariance matrices were also taken for each sample. Most of the samples showed small reproducible deviations from Gaussianity (Table III). The frequencies with the non-Gaussian noise usually coincided with a low region in the power per octave spectrum, or a very bumpy region of the spectrum. For the small non-Gaussian effects the terms of the covariance matrix were independent of sampling rate, consistent with the computer simulations for two-level systems.

Two of the samples (μSOS 1 and μSOS 3) exhibited extremely non-Gaussian noise (Table IV). The covariance matrix for μSOS 1 was reproducible throughout the six-week life of the sample, and was independent of current, as long as Johnson noise was not significant. The normalized noise variance had an unexpected sampling-rate dependence not consistent with the simple two-level systems model. The normalized noise variance increased monotonically with the number of frequency bins of the FFT contained in the octave being measured. To obtain the frequency spectrum of the noise variance it was thus necessary to take data with many different sampling rates and group the data according to the number of bins per octave (Fig. 6). The expectation of the normalized variance would be 1.0 for Gaussian noise, and for non-Gaussian noise due to a small number of two-state systems the normalized variance would not increase with the number of bins per octave. Figure 7 shows the corresponding power spectrum for this sample (μSOS 3). Figure 8 shows the frequency spectrum of the normalized noise variance for μSOS 1 at two temperatures exhibiting thermal activation, and Fig. 9 shows the corresponding power spectra. Note that the peaks in the noise variance correspond approximately with peaks in the power spectra, for μSOS 1.

This dependence of the normalized power variance on the number of bins implies a slow variation of the power. Figure 10 has a tracing of the non-Gaussian noise power over a long time scale, illustrating these slow variations for μSOS 7 together with two tracings of Gaussian noise (one from a similar $1/f$ source) with the same mean power. This tracing shows that the power modulation itself is not a simple two-level modulation nor is it obviously asymmetric.

Figure 11 shows the "second spectrum" for the most non-Gaussian noise octave of μSOS 3. This figure is normalized using the total mean-square noise power so that Gaussian noise would appear as a horizontal line at zero. Also, non-Gaussian noise due to a small number of constant-amplitude two-state systems would produce a frequency-independent spectrum. The flattening of the spectrum at higher frequencies may indicate this second type of non-Gaussianity. The data from μSOS 1 (not shown) are similar.

Because of the narrow peaks in the frequency spectra of the noise variance we were led to consider the system of

TABLE IV. Normalized covariance matrix for μSOS 1 measured from 1000 transforms. The frequency range covered is 0.5—45 Hz.

Octave	4	5	6	7	8	9	10
4	0.96						
5	0.03	1.02					
6	0.02	0.05	1.14				
7	0.06	0.05	0.05	1.14			
8	0.03	0.02	0.05	0.17	1.22		
9	0.02	0.04	0.07	0.12	0.26	2.01	
10	0.01	−0.02	0.12	0.14	0.25	0.37	1.66

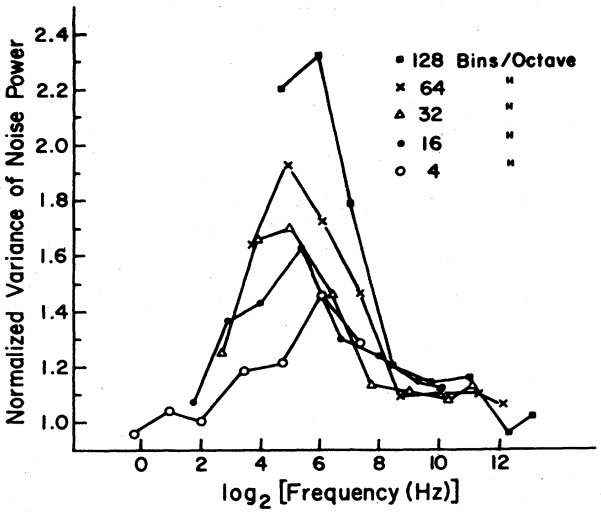

FIG. 6. Each line in the figure shows the normalized variance of the noise power of μSOS 3 as a function of frequency, with the number of frequency bands per octave held constant. The different points on a single line were obtained by changing the sampling rate. The line with the highest peak corresponds to the data in which 128 frequency bins were summed to measure the power in an octave.

an amplitude-modulated two-state system with a background of Gaussian noise. If the effect of the modulation is to produce a noise voltage from the two-state system $V_n(t)$:

$$V_n(t)=[1+Z(t)r]V(t)\ ,$$

where $V(t)$ is the unmodulated noise voltage, $r<1$ is a constant giving the magnitude of the modulation, and $Z(t)$ is a random variable with a standard normal distribution then it is simple to show that the normalized noise variance for an octave is

$$V=1+\beta^2\left[\frac{5r^2(1+N_b)}{1+r^2}\right]$$

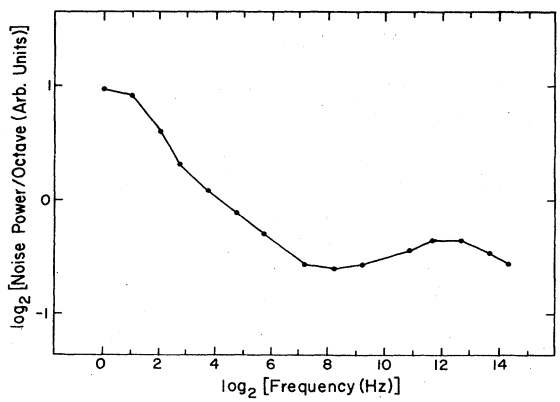

FIG. 7. Power spectrum for μSOS 3 at room temperature. Notice that the vertical axis has been expanded to emphasize deviations from the $1/f$ law.

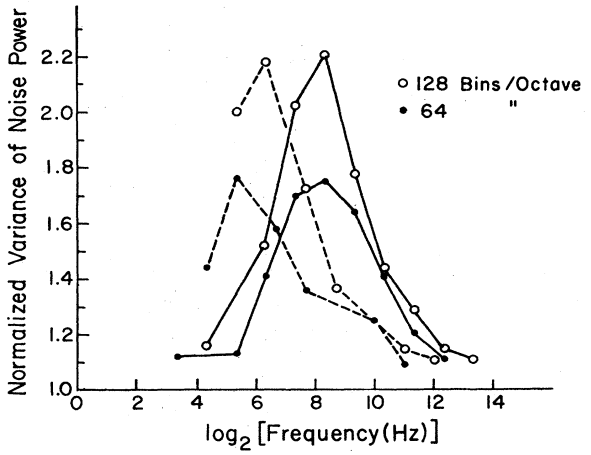

FIG. 8. Normalized variance of the noise power of μSOS 1 at two temperatures. The dashed and solid lines correspond to 22 and 50°C, respectively. The two lines at each temperature correspond to different numbers of bins per octave as in Fig. 6.

plus terms of order r^4 and higher where N_b is the number of frequency bins of the FFT summed to obtain the octave power, and β is the fraction of the total noise power in the octave caused by the modulation of the two-state system. For both μSOS 1 and μSOS 3 we have $V\cong 2.2$ at maximum so $\beta r\cong 0.043$. Thus, for example, a 21% modulation of a trap comprising 21% of the total noise would be consistent with the data.

DISCUSSION AND CONCLUSION

To a crude approximation the results confirmed the superposition of two-state systems model. Randomness in the shape of the spectra and non-Gaussian effects become observable in samples with area less than about 1 μm^2. The largest non-Gaussianity was associated with spectral features, with characteristic frequencies showing thermal activation and with temperature-dependent magnitudes. The spectral differences between samples were stable for times up to months. In all these respects we seem to be seeing simply the sort of transitions found by Ralls *et al.*[2], but in samples large enough to see the $1/f$-like net

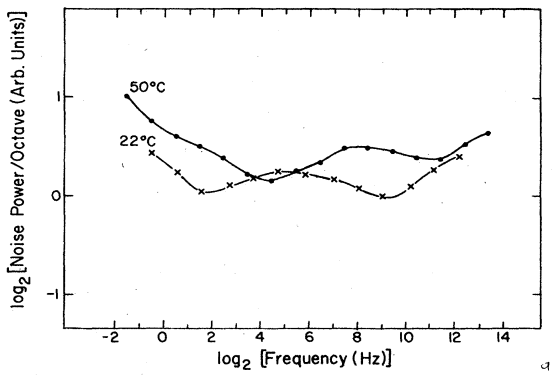

FIG. 9. Power spectra at two temperatures for μSOS 1.

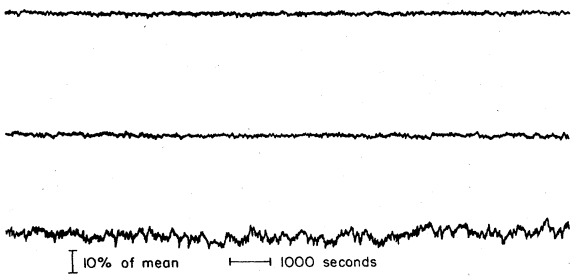

FIG. 10. Three traces show the rms noise in about one octave as a function of time. The noise voltage was filtered with a 30 Hz high-pass *RC* filter and a 30-Hz eight-pole Butterworth low-pass (Frequency Devices 901F). The filtered noise was sent to a Keithley 177 digital multimeter used as a true rms voltmeter, whose analog output was filtered at ~ 0.1 Hz and recorded. The top trace was taken from a Johnson noise source, the middle from the approximately Gaussian μSOS 7 and the bottom from the non-Gaussian μSOS 3. Each source was adjusted to about the same mean rms noise. Low-frequency noise amplitude modulations are evident in μSOS 3.

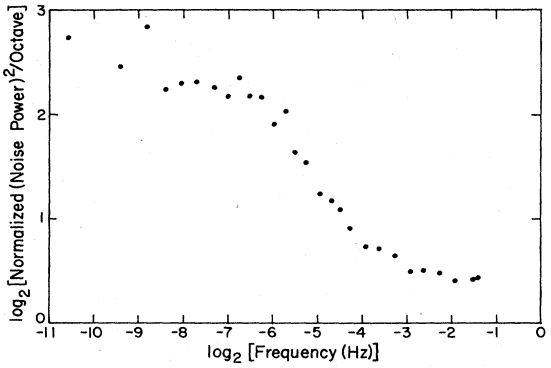

FIG. 11. "Second spectrum" of the noise for μSOS 3 at room temperature. The voltage sampling rate was 850 Hz. 64 bins of the squared FFT were summed to obtain the power in the octave 53 to 106 Hz. 80 time series of 1024 of these power measurements were again Fourier transformed, squared, and averaged to obtain this second spectrum which is normalized by dividing by the expectation for Gaussian noise.

spectrum and thus too large to directly observe single transitions. This result then helps bridge the gap between single-system measurements and the large-number Gaussian limit, indicating that there is a smooth transition. The general behavior of the RWRP is not present.

The magnitude of the non-Gaussian effects, sample-to-sample variation, and anomalous temperature dependence provide evidence about what process gives the $1/f$ kinetics. Assuming that the fractional effect of a single trap on the conductance is about equal to the inverse of the number of charge carriers (as suggested by Hall-noise measurements[1]), one finds that several traps per $(\mu m)^2$ with duty cycles not far from 0.5 with characteristic frequencies in each octave are needed to account for the $1/f$-noise magnitude. Our results are most easily fit to a model in which the transitions with the $1/f$ kinetics are the trapping-detrapping itself as in the results of Ralls *et al.*,[2] and as previously mentioned as the "tight-coupling" possibility.[1]

The nature of the coupling between the electron trapping and some lattice motions which prevents simple tunnelling from being the dominant rate is not known. However, if the observations of Ralls *et al.* are relevant also to our system, one may conclude from the field dependence of the on-off rates that the transition is adiabatic. That is, since both on and off rates showed simple exponential dependences on electric field there appears to be a transition state with the electron part way between the bulk and the trap. This contrasts with a picture in which the lattice has two well-defined states corresponding to distinct trap depths.

The most surprising result is that the details of the noise statistics definitely differed from those of a simple two-state systems model. The differences between the actual results and the model simulations indicate that the amplitudes of some prominent "two-state" components were not constant in time, but showed modulations, with the modulations having messy spectra very roughly of an $f^{-0.5}$ form, at least over a narrow frequency range. In fact, if observations had been confined to a frequency window showing such non-Gaussian effects at one temperature, the results would have looked more like an RWRP than like a two-state systems model. Slow rearrangements in the glass are the likely origin of these very slow effects, but such processes do not directly determine the $1/f$ kinetics of the ordinary spectra.

It is possible that with sufficiently clean surface regions the disorder necessary to give the $1/f$ kinetics would remain without that disorder which gives the slow modulation of the traps, but it is not likely to be simply a coincidence that the $1/f$ noise arises from a region in which its parameters can be a bit noisy on a sufficiently small scale. The $1/f$ spectrum requires a distribution of relaxation times, which is most easily explained in amorphous regions. Such regions, however, are likely to have various other slow degrees of freedom capable of modulating the effects of the transitions which directly cause the noise. It would be interesting to see whether such modulations appear in other $1/f$ systems and also whether they appear in semiconductors which show similar trapping noise but from discrete types of traps.[15,16] Such discrete traps, apparently residing in crystalline regions, might not show any modulation since, if they are not too dense, the crystal would have no obvious slow modes which could affect the trap or its coupling to the conductivity.

ACKNOWLEDGMENTS

This work was supported by National Science Foundation (NSF)-DMR Grant No. 83-04470 and through facility usage at the Materials Research Lab by NSF-DMR Grant No. 80-20250. Preliminary results were presented at the March, 1983 APS meeting.

[1]R. D. Black, P. J. Restle, and M. B. Weissman, Phys. Rev. B **28**, 1935 (1983).

[2]K. S. Ralls, W. J. Skocpol, L. D. Jackel, R. E. Howard, L. A. Fetter, R. W. Epworth, and D. M. Tennant, Phys. Rev. Lett. **52**, 228 (1984).

[3]Ia. G. Sinai, in *Proceedings of the Berlin Conference on Mathematical Problems in Theoretical Physics,* edited by R. S. Schrader, R. Seiler, and D. A. Uhlenbrock (Springer, Berlin, 1982), p. 12.

[4]E. Marinari, G. Parisi, D. Ruelle, and P. Windey, Phys. Rev. Lett. **50**, 1223 (1983), Commun. Math. Phys. **89**, 1 (1982).

[5]A. van der Ziel, in *Advances in Electronics and Electron Physics,* edited by L. Marton and C. Marton (Academic, New York, 1979), Vol. 49, p. 225.

[6]H. E. Maes and S. Usmani, J. Appl. Phys. **54**, 1937 (1983).

[7]R. D. Black, M. B. Weissman, and P. J. Restle, J. Appl. Phys. **53**, 6280 (1982).

[8]K. Zheng, K. Duh, and A. van der Ziel, Proceedings of the 7th International Conferences on Noise in Physical Systems, Montpelier, 1983 (unpublished).

[9]P. Dutta and P. M. Horn, Rev. Mod. Phys. **53**, 497 (1981).

[10]The temperature dependence and logarithmic spectra corrections in Ref. 4 do not obey a Dutta-Horn relation. We believe that the temperature dependence is correct but that a slight error was made in the logarithmic spectral corrections, which ought to go as $[\ln(\gamma f_{\max}/f]^3$ rather than $[\ln(\gamma f_{\max}/f]^4$, where γ is an adjustable dimensionless parameter (roughly 20) and $f_{\max}$ is the stepping attempt rate. Our result actual fits their simulations (their Fig. 4) better than the quartic correction, which was derived by incorrectly neglecting the absence of scaling at $f_{\max}$.

[11]M. Nelkin and A.-M. S. Tremblay, J. Stat. Phys. **25**, 253 (1981).

[12]P. J. Restle, M. B. Weissman, and R. D. Black, J. Appl. Phys. **54**, 5844 (1983).

[13]D. S. Fisher (unpublished).

[14]A. B. Glaser and G. E. Subak-Sharpe, *Integrated Circuit Engineering* (Addison-Wesley, Reading, 1977), p. 203.

[15]L. Loreck, H. Dämbkes, K. Heime, K. Ploog, and G. Weimann, in *Noise in Physical Systems and* $1/f$ *Noise,* edited by M. Savelli, G. Lecoy, and J.-P. Nougier (North-Holland, Amsterdam, 1983), p. 261.

[16]K. Kandiah, in *Noise in Physical Systems and* $1/f$ *Noise,* edited by M. Savelli, G. Lecoy, and J.-P. Nougier (North-Holland, Amsterdam, 1983), p. 287.